Global hyperon polarization in Au+Au collisions at $\sqrt{s_{NN}} = 27$ GeV in the STAR experiment

Egor Alpatov (for the STAR collaboration)

National Research Nuclear University MEPhI, Russia, Moscow

E-mail: egroker1@gmail.com

Abstract. The Quark-Gluon Plasma (QGP), appearing in non-central nucleus-nucleus collisions is generated with large orbital angular momentum. Spin-orbit coupling aligns spin directions of produced particles with the system angular momentum, through the creation of local vorticity. Properties of hyperon weak decays lead to the way of measuring polarization, that reflects vorticity.

The global polarization of Λ and $\overline{\Lambda}$ hyperons was measured for Au+Au collisions at $\sqrt{s_{NN}} =$ 7.7 - 200 GeV recorded with the STAR at the RHIC. However, different theoretical approaches are still in need of new experimental input to describe global polarization properly. That's why it is important to measure the global polarization of different particle species. In this talk, we will report new results of hyperon global polarization ($P_{\Lambda+\overline{\Lambda}}$ and $P_{\Xi^-+\overline{\Xi}^+}$) measurement via different methods for high-statistics Au+Au collisions at $\sqrt{s_{NN}} = 27$ GeV.

1. Introduction

Experiments at the Relativistic Heavy Ion Collider (RHIC) and Large Hadron Collider have been exploring the properties of the partonic matter state, the quark-gluon plasma (QGP) since their early days of operation. The collective behavior of QGP was one of the most important discoveries, which led to the possible conclusion that system is a liquid with very specific low viscosity [1].

Extensive hydrodynamic model studies have successfully described main features of these collective phenomena, however, observations such as directed azimuthal anisotropic flow still cannot be quantitavely described. Investigations are in progress and one of the possible important ingredients to understand directed flow measurements could be an improved knowledge of initial conditions — particularly along the longitudinal or rapidity direction. [2, 3]. Measurements such as hyperon global polarization can lead to better understanding of both the fluid properties of the medium and the longitudinal structure of the initial state.

Model studies of non-central collisions suggested evidences for vortical structure in the QGP, appearing due to initial angular momentum of the system [4, 5]. This provides a possible explanation of the globally polarized particles that were observed by the STAR experiment [6]. Global polarization was measured with hyperons weak decays, in which the baryon is preferentially emitted in the parent hyperon spin direction (and in opposite direction for antiparticles).

In the hyperon decays the angular distribution of daughter baryons in the parent hyperon

rest frame is given by:

$$\frac{dN}{d\cos\theta^*} \propto 1 + \alpha_H P_H \cos\theta^*, \tag{1}$$

α_H is the hyperon decay parameter, P_H is the hyperon global polarization, $\cos\theta^*$ is the angle between the polarization vector and daughter baryon momentum in the hyperon rest frame. The polarization of hyperons should be measured with respect to the reaction plane (which is defined by the beam direction and impact parameter vector) because of perpendicularity of system angular momentum to this plane [7].

Global Λ polarization results by the STAR Collaboration for Au+Au collisions were published for $\sqrt{s_{NN}}$ = 7.7-200 GeV [8, 9]. While most of the theoretical calculations can quantitively explain the energy dependence of the Λ polarization [10, 11, 12], many of them fail to explain differential measurements like p_T or η dependencies. New physical inputs are needed for further researches of global polarization nature, and this could be achieved by additional measurements of multistrange hyperons global polarization.

In this talk, we report on the measurements of the global polarization of $\Xi^- + \bar{\Xi}^+$ hyperons in Au+Au collisions at $\sqrt{s_{NN}}$ = 27 GeV and compare it to that of $\Lambda + \bar{\Lambda}$.

2. Data analysis

Dataset of Au+Au collisions at $\sqrt{s_{NN}} = 27$ GeV collected in 2018 by STAR experiment [13] was used for this analysis. More than 400 million events with the collision vertex within 70 cm of the center of Time Projection Chamber (TPC) that passed minimum-bias trigger were analyzed. The vertex position in the transverse plane was limited to be within 2 cm from the beam line.

Charged-particle tracks were measured in the TPC within a pseudorapidity range $|\eta| < 1$ and with full azimuthal acceptance. Tracks with momentum > 0.15 GeV/c were identified via ionization energy losses, dE/dx, and were used for hyperon reconstruction. The collision centrality was determined based on the measured multiplicity of charged tracks within midrapidity region and this was matched to a Monte Carlo Glauber simulation [14].

2.1. Event plane reconstruction

Event plane detectors (EPD) and Beam-Beam Counters (BBC) were used separately for event plane angle calculations, as a proxy for the reaction plane angle.

Global polarization can be measured with respect to the reaction plane, which was estimated as the true first-order event plane, Ψ_1, determined by EPD ($2.1 < \eta < 5.1$) and BBC ($3.3 < \eta < 5.1$). Both detectors are based on scintillators embedded with wavelength-shifting fibers (372 tiles in 16 rings for EPD and 18 tiles in 2 rings for BBC). Measured ADC signal from silicon photomultipliers was used as a weight to calculate Q-vectors:

$$Q_{n,x} = \frac{\sum w_i \cos(n\phi_i)}{\sqrt{\sum w_i}}, \tag{2}$$

$$Q_{n,y} = \frac{\sum w_i \sin(n\phi_i)}{\sqrt{\sum w_i}}, \tag{3}$$

$$\psi_n = \frac{1}{n}\,\mathrm{atan2}(Q_{n,y}, Q_{n,x}). \tag{4}$$

The event plane resolution, $Res(\Psi_1) = \left\langle \cos\left(\Psi_1 - \Psi_1^{obs}\right)\right\rangle$, was estimated using two-subevent method [7], where Ψ_1^{obs} denotes the measured event plane. Figure 1 shows the comparison between EPD and BBC resolutions. EPD resolution is about 1.5 times larger than that for BBC due to wider acceptance and better granularity.

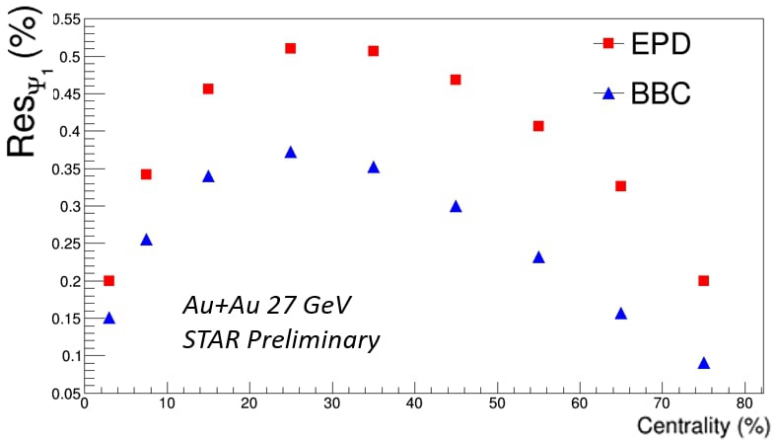

Figure 1. Resolution of the first-order event plane determined by EPD and BBC separately in Au+Au collisions at $\sqrt{s_{NN}} = 27$ GeV.

2.2. Hyperon reconstruction

Tracks from TPC were used as daughter particle candidates for hyperon reconstruction with the following requirements. The number of associated ionization hits in TPC was required to be greater than 15. Transverse momentum of tracks was required to be greater than 0.15 GeV/c and pseudorapidity of tracks to lie in range of $|\eta| < 1$.

The parent Ξ^- ($\bar{\Xi}^+$) candidates were reconstructed via their decays to $\Lambda + \pi^-$ ($\bar{\Lambda} + \pi^+$), and daughter hyperons were reconstructed in $\Lambda \to p + \pi^-$ ($\bar{\Lambda} \to \bar{p} + \pi^+$) decays.

Reconstruction of hyperons was performed based on the Kalman Filter method developed for the CBM and ALICE experiments [15]. In addition, hyperons were reconstructed via traditional method based on decay topology [8].

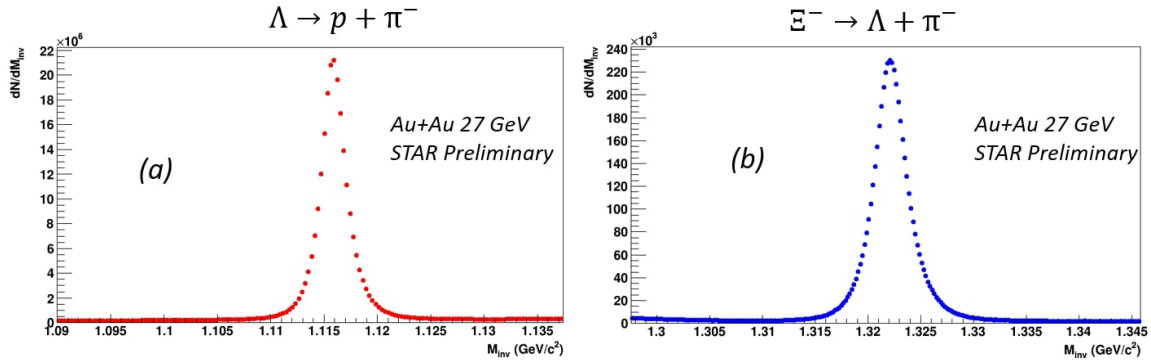

Figure 2. Invariant mass distributions for $p\pi^-$ (a) and $\Lambda\pi^-$ (b) pairs measured in Au+Au collisions at $\sqrt{s_{NN}} = 27$ GeV.

2.3. Polarization measurement

The first-order event plane, Ψ_1, allows one to estimate the direction of the initial angular momentum. Global polarization projected onto the direction of the system global angular momentum after incorporating the event plane resolution could be estimated as:

$$P_H = \frac{8}{\pi \alpha_H} \frac{\left\langle sin(\Psi_1^{obs} - \phi^*_{daughter}) \right\rangle}{Res(\Psi_1)}, \tag{5}$$

where $\phi^*_{daughter}$ is the azimuthal angle of the daughter baryon in the parent hyperon rest frame. Decay parameter values are $\alpha_\Lambda = 0.732 \pm 0.014$, $\alpha_{\bar{\Lambda}} = -0.758 \pm 0.010$, $\alpha_{\Xi^-} = -\alpha_{\bar{\Xi}^+} = -0.401 \pm 0.010$ [16].

Two methods that were used to measure the Ξ polarization are as follows. The Ξ global polarization was measured directly using Λ azimuthal angle in the Ξ rest frame. Also Ξ polarization was estimated from the Λ daughter polarization with transfer factor to be $C_{\Xi^-\Lambda} = 0.932$ [17].

The invariant mass method was used for signal (P_H) extraction [18]. Mean value of the sine term in Eq. (5) was measured as a function of daughter's pair invariant mass. Observed signal is the sum of real hyperons polarization and background polarization:

$$< sin(\Psi_1 - \phi^*_p) >^{obs} = f^{sgn}(M_{inv}) < sin(\Psi_1 - \phi^*_p) >^{sgn} + \\ + f^{Bg}(M_{inv}) < sin(\Psi_1 - \phi^*_p) >^{Bg}, \tag{6}$$

where $f^{Bg}(M_{inv})$ is the invariant mass distribution of the background fraction. The data were fitted with Eq. (6) to extract the $< \sin(\Psi_1 - \phi^*_{daughter}) >^{sgn}$, which is the polarization signal of hyperons.

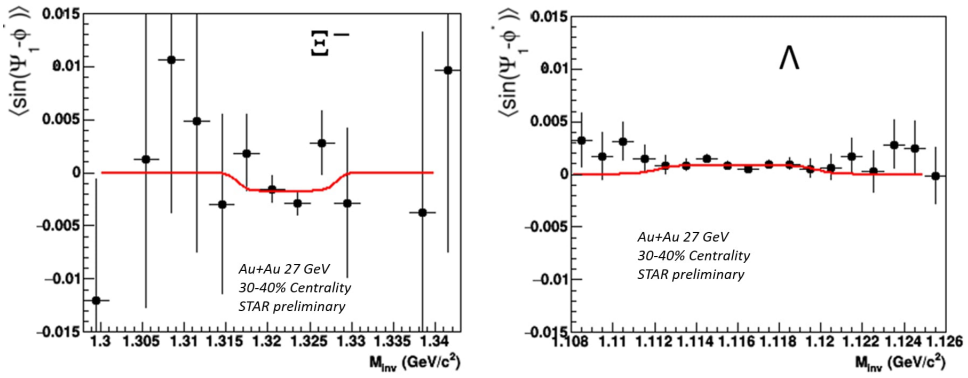

Figure 3. $< \sin(\Psi_1 - \phi^*_{daughter}) >$ as a function of the invariant mass for Ξ^- and Λ in the 30-40% central Au+Au collisions at $\sqrt{s_{NN}} = 27$ GeV. Red line corresponds to the fit using Eq. (6).

Figure 3 shows the observed $< \sin(\Psi_1 - \phi^*_{daughter}) >$ as a function of invariant mass. The mean sine-component of the background was assumed to be zero due the high purity of the hyperons sample. The systematic uncertainty associated with this assumption will be evaluated in future.

3. Results

The global polarization of Λ and the new measurements of Ξ polarization at $\sqrt{s_{NN}} = 27$ GeV as a function of collision energy are presented in Fig. 4. The results of this analysis are shown together with previous studies at $\sqrt{s_{NN}} = 7.7$-39 GeV [8], the 2018 result at $\sqrt{s_{NN}} = 200$ GeV [9] and the preliminary results presented at the Quark Matter 2019 conference for $\Lambda + \bar{\Lambda}$ at

$\sqrt{s_{NN}}$ = 27 and 54.4 GeV. Previous results for Λ were rescaled due to new decay parameter values [16], $\frac{\alpha_{\Lambda old}}{\alpha_{\Lambda new}} = 0.869$.

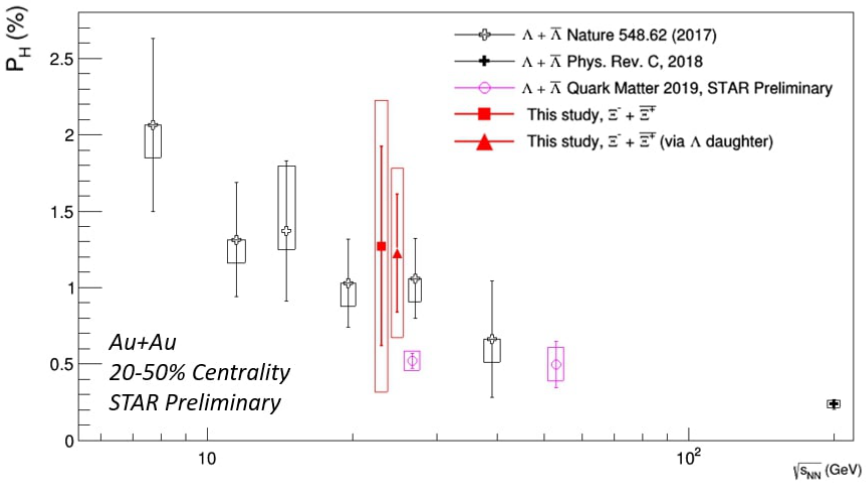

Figure 4. Global polarization of $\Lambda + \bar{\Lambda}$ and $\Xi^- + \bar{\Xi}^+$ as a function of collision energy $\sqrt{s_{NN}}$ for 20-50% centrality Au+Au collisions. Open boxes and vertical lines show systematic and statistical uncertainties, respectively. Note that the data points at plot for different energies are slightly horizontally shifted for visibility.

The centrality dependence of Ξ global polarization was measured as a part of this study. Figure 5 shows the comparison of Ξ global polarization as a function of collision centrality with the same for Λ polarization. Weak centrality dependence of Ξ polarization is seen. This and other possible differential measurements would require more statistics in further experiments.

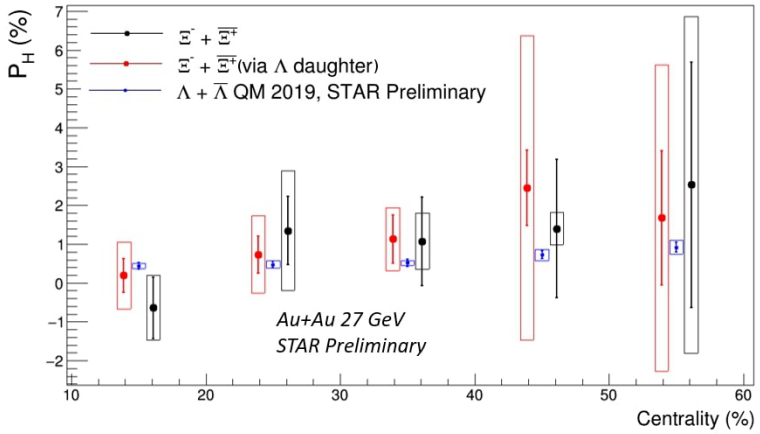

Figure 5. Global polarization of $\Lambda + \bar{\Lambda}$ and $\Xi^- + \bar{\Xi}^+$ as a function of centrality of Au+Au collisions at $\sqrt{s_{NN}}$ = 27 GeV. Open boxes and vertical lines show systematic and statistical uncertainties, respectively.

Systematic uncertainties estimation included usage of decay topology instead of Kalman

Filter method, Event-Plane signal extraction method [9], and variation of mass window for Ξ reconstruction.

4. Summary

We present the first results of global polarization measurements for $\Xi^- + \bar{\Xi}^+$ in Au+Au collisions at $\sqrt{s_{NN}} = 27$ GeV. Global polarization was measured for Ξ hyperons directly and via transfer to decay daughters. A weak centrality dependence was seen within uncertainties.

A non-zero signal for Ξ global polarization was observed for 20-50% centrality region. Results of directly measured Ξ global polarization and via Λ daughters are consistent within given large uncertainty. The values of Ξ hyperon global polarization are consistent with that of Λ hyperon measurement.

Acknowledgements

The work was supported by the Ministry of Science and Higher Education of the Russian Federation, Project "Fundamental properties of elementary particles and cosmology" No 0723-2020-0041, and by the National Research Nuclear University MEPhI in the framework of the Russian Academic Excellence Project (contract No. 02.a03.21.0005, 27.08.2013).

References

[1] Voloshin S, Poskanzer A, Snellings R 2010 *Landolt-Bornstein* **23** 293-333
[2] Adamczyk L *et. al* 2014 *Phys.Rev.Lett.* **112** 162301
[3] Bozek P, Wyskiel I 2010 *Phys.Rev.*C **81** 054902
[4] Liang Z, Wang X 2005 *Phys. Rev. Lett.* **94** 102301
[5] Voloshin S 2004 *arXiv nucl-th/0410089*
[6] Abelev B 2007 *Phys.Rev.*C **76** 024915
[7] Voloshin S, Niida T 2016 *Phys.Rev.*C **94** 021901
[8] Adamczyk L *et. al* 2017 *Nature* **548** 62–65
[9] Adam J *et. al* 2018 *Phys.Rev.*C **96** 14910
[10] Kharzeev D, Liao J, Voloshin S, Wang G 2016 *Prog.Part.Nucl.Phys.* **88** 1-28
[11] Baznat M, Gudima K, Sorin A, Teryaev O 2018 *Phys.Rev.*C **97** 041902
[12] Karpenko I, Becattini F 2017 *The European Physical Journal* C **77** 10
[13] Ackermann K *at. al* 2003 *Nucl.Instrum.Meth.*A **499** 624–632
[14] Adamczyk L *et. al* 2012 *Phys.Rev.*C **86** 054908
[15] Zyzak M 2016 *Online selection of short-lived particles on365 many-core computer architectures in the CBM experiment at FAIR, Ph.D. thesis, Johann Wolfgang Goethe-367 Universitat*
[16] Zyla P *et. al* 2020 *Review of Particle Physics PTEP* **2020** 083C01
[17] Lee T, Yang C 1957 *Phys.Rev.* **108** 1645–1647
[18] Adamczyk L *et. al* 2013 *Phys.Rev.*C **88** 014902